Phase II Trial of Atezolizumab and Bevacizumab for Treatment of HPV-Positive Unresectable or Metastatic Squamous Cell Carcinoma of the Anal Canal

Van K. Morris[1], Suyu Liu[2], Kangyu Lin[1], Haifeng Zhu[3], Seema Prasad[1], Armeen Mahvash[4], Priya Bhosale[4], Baohua Sun[5], Edwin R. Parra[5], Ignacio Wistuba[5], Arjun Peddireddy[6], James Yao[1], Julia Mendoza-Perez[5], Mark Knafl[3], Scott E. Woodman[3], Cathy Eng[7], and Daniel Halperin[1]

ABSTRACT

Purpose: Anti–PD-L1 antibodies are associated with responses in <25% of patients with metastatic human papillomavirus–associated malignancies. VEGF signaling causes immune evasion and immune suppression within the tumor. We evaluated the anti–PD-L1 antibody atezolizumab and anti-VEGF antibody bevacizumab for patients with unresectable, advanced anal cancer.

Patients and Methods: For this phase II study, participants with previously treated, immunotherapy-naïve anal cancer received atezolizumab (1,200 mg) and bevacizumab (15 mg/kg) intravenously every 21 days. Responses were evaluated every 9 weeks (RECIST version 1.1). The primary endpoint was the best radiographic response. Median survival was estimated by Kaplan–Meier and compared for selected biomarkers (including paired pre- and on-treatment biopsies) using a log-rank test.

Results: Among 20 participants, the overall response rate was 11% [95% confidence interval (CI): 1.2–32]. Median progression-free survival and overall survival were 4.1 months (95% CI, 2.6–not assessable) and 11.6 months (95% CI, 9.5–20), respectively. One grade 5 bevacizumab-related bowel perforation occurred. Analyses of 16 paired biopsies linked increases in IFN-γ ($P = 0.03$) and inflammatory response ($P = 0.02$) gene expression signatures with prolonged progression-free survival, as did increases in $CD3^+CD8^+PD1^+$ ($P = 0.02$) cells and decreases in $CD3^+FoxP3^+$ cells ($P = 0.04$) from 10 paired biopsies with multiplex immunofluorescence. A subgroup of anal cancers characterized by the SBS31 "prior-platinum" signature demonstrated shorter median overall survival (HR, 6.3; 95% CI, 1.2–32; $P = 0.01$).

Conclusions: Atezolizumab and bevacizumab demonstrate activity similar to anti–PD-1 antibodies alone for unresectable anal cancer. Our translational data identify undescribed chromosomal and transcriptomic biomarkers associated with survival for metastatic anal cancer. These correlative findings warrant confirmation and further validation in larger, prospective immunotherapy trials for advanced anal cancer.

Introduction

The incidence of squamous cell carcinoma of the anorectum continues to increase (1, 2). Over the past two decades, the relative proportion of patients presenting with advanced or metastatic disease at the time of their initial diagnosis for anal cancer has steadily increased (3). Most anal cancers are linked to prior infection with the human papillomavirus (HPV), most commonly HPV-16 and HPV-18 (4, 5). The most utilized treatments for patients with metastatic anal cancer have been cytotoxic chemotherapy (6–9). More recently, clinical trials evaluating antibodies against immune checkpoints like anti–PD-L1 have reported overall response rates (ORR) between 10% and 24% for patients with treatment-refractory metastatic anal cancer (10–13). There remains a paucity of effective treatment options in this setting.

VEGF not only promotes the development of new blood vessel formation to growing tumors (14, 15) but also modulates the tumor microenvironment by recruiting T cell–suppressive myeloid-derived stem cells (16). Preclinical models have suggested that blockade of VEGF may augment the immune activation state within the tumor microenvironment by increasing cytotoxic T-cell infiltration (17), removing myeloid-derived stem cells (18), and reducing immune-suppressing cytokines (19). We conducted a phase II trial evaluating the anti–PD-L1 antibody atezolizumab with the anti-VEGF antibody bevacizumab for patients with previously treated, HPV-positive, unresectable squamous cell carcinoma of the anorectum.

Patients and Methods

Study participants

Patients with histologically confirmed squamous cell carcinoma of the anus or rectum that was either metastatic and/or locally advanced and was not amenable to complete surgical resection were eligible. Patients must have had an anorectal tumor that was

[1]Department of Gastrointestinal Medical Oncology, The University of Texas – MD Anderson Cancer Center, Houston, Texas. [2]Department of Biostatistics, The University of Texas – MD Anderson Cancer Center, Houston, Texas. [3]Department of Genomic Medicine, The University of Texas – MD Anderson Cancer Center, Houston, Texas. [4]Department of Radiology, The University of Texas – MD Anderson Cancer Center, Houston, Texas. [5]Department of Translational Molecular Pathology, The University of Texas – MD Anderson Cancer Center, Houston, Texas. [6]McGovern Medical School at UT Health, Houston, Texas. [7]Vanderbilt-Ingram Cancer Center, Nashville, Tennessee.

Corresponding Author: Van K. Morris, Department of Gastrointestinal Medical Oncology, University of Texas – MD Anderson Cancer Center, 1400 Holcombe Boulevard, Unit 426, Houston, TX 77030. E-mail: vkmorris@mdanderson.org

Clin Cancer Res 2025;31:1657–66

doi: 10.1158/1078-0432.CCR-24-1512

Translational Relevance

Dual targeting of VEGF and PD-L1 with atezolizumab and bevacizumab did not seem to improve clinical outcomes beyond preceding studies with anti–PD-L1 therapies alone for patients with incurable anal cancer. Analyses of paired biopsies—historically not available in previous clinical trials for this rare malignancy—identified increases in immune activation signatures of IFN-γ and inflammatory response in association with longer survival on immunotherapy. Orthogonal confirmation using multiplex immunofluorescence showed that dynamic recruitment of cytotoxic T cells and exclusion of regulatory T cells from the tumor microenvironment for anal cancer were linked to more favorable outcomes after exposure to atezolizumab and bevacizumab. Discovery of novel chromosomal biomarkers in chromosomes 3 and 11, as well as the SBS31 "prior platinum chemotherapy" signature, was associated with survival outcomes and extended the translational profiling of anal cancers beyond genomic biomarkers following treatment with immunotherapy and bears further testing in future prospective trials.

determined to be "HPV-positive" by expression of p16 by IHC and/or detection of high-risk HPV oncogenes by DNA *in situ* hybridization in a Clinical Laboratory Improvement Amendments–approved laboratory. Prior systemic treatment was required. All eligible patients must have been at least 18 years of age, have an Eastern Cooperative Oncology Group performance status of 0 or 1, and adequate hematologic, renal, and hepatic function at study consent. Gender was self-reported by each study participant. Participants living with human immunodeficiency virus were eligible to participate provided that their $CD4^+$ T-cell count exceeded 400 cells/mm^3.

Prior treatment with immune checkpoint blockade therapies was not permitted. Patients with active or a history of autoimmune disease were not eligible for this study. Exposure to systemic immunosuppressive medications within 2 weeks of anticipated treatment initiation was not allowed. Given the known toxicity profile of bevacizumab, participants could not have a major surgical procedure within 4 weeks of the start of study treatment, significant cardiovascular disease, uncontrolled hypertension, evidence of a bleeding diathesis, or a history of a fistula or gastrointestinal perforation in the preceding 6 months.

This clinical trial (NCT03074513) received approval from the Institutional Review Board at the University of Texas MD Anderson Cancer Center prior to the start of study enrollment. Informed written consent was obtained from each study participant prior to treatment initiation and for any additional procedures in the study. All conduct for this clinical trial occurred in accordance with the Declaration of Helsinki.

Drug administration and study design

Participants received atezolizumab (1,200 mg) and bevacizumab (15 mg/kg) intravenously every 21 days until demonstration of disease progression, unacceptable toxicity, withdrawal of consent for study participation, or death (whichever came first). There was no randomization of treatment assignment for this single-arm study, and therefore, neither patient nor investigator was blinded to study treatment. Adverse events were assessed according to CTCAE version 4.0 (20) prior to every treatment dosing. Radiographic response to treatment was evaluated every 9 weeks using computerized tomography or magnetic resonance imaging per RECIST version 1.1 criteria. All enrolled patients were treated in the study, and there was no study attrition.

Study statistics

The primary endpoint for this study was best overall response—partial response or complete response—radiographically. The goal was to estimate the ORR and its 95% confidence interval (CI) using the Clopper and Pearson method. When the sample size was 20 and ORR was 0.3, the two-sided 95% exact CI would be (0.119–0.543), with a response rate of no treatment expected to be less than 5%. If the ORR was 10% and 20%, the 95% CI of ORR would be (0.012, 0.317) and (0.057, 0.437), respectively. Secondary endpoints included progression-free survival (PFS), overall survival (OS), duration of response, and occurrence of treatment-related adverse events. Disease control was defined as having a complete response, partial response, or stable disease as the best radiographic response to atezolizumab + bevacizumab, and the disease control rate was estimated according to the proportion of patients achieving disease control in this study. Participants' demographic, clinical, and pathologic features were summarized using descriptive statistics. Median time-to-event outcomes were estimated according to the Kaplan–Meier method. Differences in survival among selected clinically and molecularly annotated classifications were assessed using two-sided log-rank tests. Univariate Cox proportional hazards regression models were used to estimate and evaluate effect sizes of risk factors on survival (R version 3.4.2). A Wilcoxon test was used to compare continuous variables for different clinical and pathologic features, and a Fisher's exact *t* test was used to assess for any association between categorical variables.

Biomarker analyses

Tissue biopsies were collected from each participant within 7 days prior to treatment initiation ("pretreatment") and 3 weeks following the first dose of atezolizumab and bevacizumab ("on-treatment"). There were adequate tissue samples available for the performance of whole-exome sequencing and copy-number changes in 20/20 (100%) participants, transcriptome profiling from paired biopsies in 16/20 (80%) participants, and multiplex immunofluorescence (mIF) from paired biopsies in 10/20 (50%) participants (Supplementary Table S1). Given the historical precedent PFS estimates for anti–PD-L1 therapies as monotherapy of approximately 2 months and the median PFS of atezolizumab and bevacizumab reported at 4 months here, we became interested in exploring biomarkers associated with prolonged survival outcomes in these correlative studies. We named a PFS of greater than 6 months as "prolonged PFS" with atezolizumab and bevacizumab and an OS greater than 12 months on study as "prolonged OS" as cutoffs for evaluating selected biomarkers prognostically in this cohort.

RNA-seq FASTQ files were first processed using FastQC to evaluate the quality of sequencing reads at both the base and read levels. RNA reads were aligned to the GRCh37/hg19 genome assembly using STAR (21). Aligned RNA reads were quantified using HTSeq-count (22) and normalized into fragments per kilobase of transcript per million mapped reads (FPKM). The FPKM values were then $\log_2$-transformed for subsequent analysis. For gene expression and gene set enrichment analysis, the gene expression differences between only paired baseline and posttreatment samples were calculated and then compared in groups. For identifying the

differentially regulated genes between patients of longer versus shorter PFS and OS, we employed the "limma trend" mode available in the limma package. Genes with an adjusted *P* value below 0.05 were considered as differentially regulated genes.

Gene set enrichment analysis was conducted with the fast gene set enrichment algorithm from the R package "fgsea" (version 1.16.0). We utilized two gene sets for enrichment analysis: the "hallmark" gene set, which includes 50 gene sets that represent well-defined biological states or processes, and the "nano signaling pathway" gene set, which includes genes involved in nanomaterial–cell interactions and signaling pathways (23). For each gene set, we computed enrichment scores for all samples using the default parameters in fgsea. *P* values were corrected for multiple testing using the Benjamini–Hochberg method.

Copy-number analysis

The tumor sample purity and ploidy estimates were calculated using Sequenza algorithms. CBS (or HMM)-derived segmented copy-number values were corrected using the *In Silico* Admixture Removal procedure (24). Subsequently, significant focal copy number alterations were identified from the ISAR-corrected segmented data using GISTIC 2.0.225. The following parameters were used: amplification threshold: 0.3, deletion threshold: 0.3, focal length cutoff: 0.70, gene GISTIC: yes, confidence level: 0.99, *q*-value threshold: 0.25, join segment size: 4, remove X: no, cap val: 1.5, run broad analysis: yes, max sample segs: 2,000, arm peel: yes, gene collapse method: extreme. Tumors were then clustered based on thresholded copy number at reoccurring alteration peaks from GISTIC analysis.

Table 1. Patient demographics and clinical characteristics.

Patient characteristics (*N* = 20)	Number (%)
Age, median (years, range)	59 (43–80)
Gender	
Female	17 (85)
Male	3 (15)
Timing of metastatic presentation	
Metachronous	7 (35)
Synchronous	13 (65)
Number of metastatic treatment lines	
1	12 (60)
2	4 (20)
3	2 (10)
4	1 (5)
6	1 (5)
Liver metastases	
Yes	12 (60)
No	8 (40)
Lung metastases	
Yes	11 (55)
No	9 (45)
Distant lymph node metastases	
Yes	10 (50)
No	10 (50)
Unresectable pelvic tumor	
Yes	4 (20)
No	16 (80)

Whole-exome sequencing data processing and analysis

FASTQ files were aligned to the reference genome GRCh37/hg19 using BWA (25). The aligned BAM files were subjected to mark duplication, realignment, and recalibration using Picard and GATK (26) before any downstream analyses. Somatic variant and copy-number alterations were performed as previously described (27). Somatic mutations and short insertions/deletions were called and postfiltered using the Mutect2 (28) module of GATK and Pindel (29), respectively. Identified variants were then annotated to genes, transcripts, and variant severity using Annovar (30). Somatic copy-number alterations in tumor were identified from WES data using HMMCopy (31). Segmented data were processed using GISTIC2 (32). Cell purity and ploidy were estimated from WES data using Sequenza (33). Single-nucleotide variant mutational signatures were extracted from the COSMIC database using the MutationalPatterns R package (34). In brief, a trinucleotide (single-nucleotide variant + upstream/downstream neighboring nucleotide) mutation count matrix was calculated, and then the mutational signature and the relative contribution matrix of each signature were extracted from the trinucleotide matrix using nonnegative matrix factorization (R package). The derived mutational signature was refitted into well-known COSMIC somatic single-base substitutions (SBS) mutational signatures (https://cancer.sanger.ac.uk/signatures/sbs/). Unsupervised clustering of the relative contribution matrix was conducted and visualized using the R package ComplexHeatmap.

mIF staining and image analysis

mIF staining was performed using a similar method previously described (35). Briefly, four μm–thick formalin-fixed, paraffin-embedded sample sections were stained using an mIF panel that contained antibodies against pancytokeratin (clone AE1/AE3, RRID:AB_2631307, dilution 1:50, Dako), CD3 (polyclonal, RRID:AB_2721019, dilution 1:100, Dako), CD8 (clone C8/144B, RRID:AB_11000353, dilution 1:25, Thermo Fisher Scientific), FOXP3 (clone D2W8E, RRID:AB_2747370, dilution 1:100, Cell Signaling Technology), PD-1 (clone EPR4877-2, RRID:AB_2894867, dilution 1:250, Abcam), PD-L1 (clone E1L3N, RRID:AB_2687655, dilution 1:250, Cell Signaling Technology), KI67 (clone MIB-1, RRID:AB_2142367, dilution 1:100, Dako), and CD68 (clone PG-M1, RRID:AB_2074844, dilution 1:25, Dako). All the markers were stained in sequence using their respective fluorophore contained in the Opal 7 IHC kit (Akoya Biosciences) and the individual tyramide signal amplification fluorophores Opal Polaris 480 and Opal Polaris 780 kits (Akoya Biosciences). The slides were scanned using the Vectra Polaris 1.0.13 (Akoya Biosciences) at low magnification, 10× (1.0 μm/pixel) through the complete emission spectrum and using positive tonsil controls from the run staining to calibrate the spectral image scanner protocol. A pathologist selected all the tumor areas using regions of interest for scanning in high magnification by the Phenochart Software image viewer 1.0.12 (931 × 698 μm size at resolution 20×) to capture various elements of tissue heterogeneity. A pathologist analyzed each region of interest using inForm 2.4.8 image analysis software (Akoya Biosciences). Marker colocalization was used to identify specific tumor and stroma compartment cell phenotypes. The densities of each cell phenotype were quantified, and the final data were expressed as the number of cells/mm^2. The data were consolidated using R Studio 3.5.3 (phenoptr 0.2.2 packet; https://rdrr.io/github/akoyabio/phenoptrReports/f/, Akoya Biosciences).

RNA-seq data processing and analysis

RNA-seq FASTQ files were first processed using FastQC to evaluate the quality of sequencing reads at both the base and read

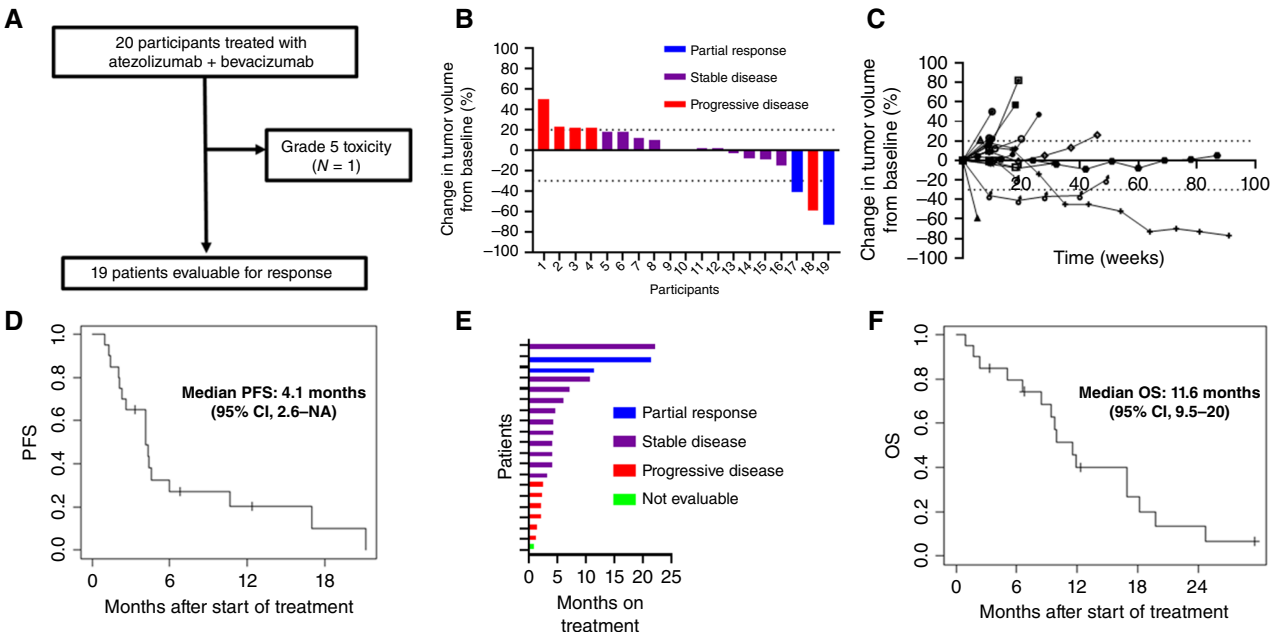

Figure 1.
Consort diagram (**A**), waterfall plot (**B**), spider plot (**C**), PFS (**D**), swimmer's plot (**E**), and OS (**F**) for atezolizumab and bevacizumab.

levels. RNA reads were aligned to the GRCh37/hg19 genome assembly using STAR (21). Aligned RNA reads were quantified using HTSeq-count (22) and normalized into FPKM. The FPKM values were then $\log_2$-transformed for subsequent analysis. Limma was used to identify differentially expressed genes between patients with longer versus shorter median PFS and OS. For gene set enrichment analyses, the hallmark gene sets (version 7.4) and nanostring signaling pathways were downloaded and analyzed using the fgsea software package.

Data availability

Raw data for this study were generated at the University of Texas MD Anderson Cancer Center. The data reported in this study are based on the use of study data from consented participants that we have uploaded on the dbGaP website, under dbGaP accession phs003845.v1.p1. Requests for additional data can be directed to the corresponding author.

Results

Clinical activity

Twenty patients (**Table 1**; Supplementary Table S2 for Study Representativeness) with HPV-positive, metastatic, or unresectable squamous cell carcinoma of the anorectum were treated with atezolizumab and bevacizumab (**Fig. 1A**). The median number of prior lines of treatment for advanced anal cancer was 1 (range, 1–6). The median number of doses of atezolizumab and bevacizumab was 6 (range, 2–30). One patient was not evaluable for treatment response due to a grade 5 bowel perforation prior to the first restaging. After a median follow-up time of 9.6 months (range, 3.3–29.6 months), there were two patients with partial responses radiographically. Among 19 patients evaluable for response (**Fig. 1B**; Supplementary Table S1 for details between demographics and response to treatment), the ORR was 11% (95% CI, 1–33). With an ORR less than 30%, the primary objective for clinical efficacy was not met. There were 11 patients who had stable disease as their best response, and the disease control rate was 68% (95% CI, 43–87). Both partial responses were confirmed on subsequent imaging studies (**Fig. 1C**). Per **Fig. 1D**, the median PFS was estimated at 4.1 months (95% CI, 2.6–not achieved). Two patients remained on study beyond 20 months (**Fig. 1E**). Previous radiation treatment was not linked to the PFS outcome (HR, 0.52; 95% CI, 0.19–1.45; $P = 0.21$). There were no other clinical or pathologic factors that were significantly associated with PFS (Supplementary Table S3).

Median OS (**Fig. 1F**) was estimated at 11.6 months (95% CI, 9.5–19.8). One- and two-year OS rates were 40% (95% CI, 23–71) and 13% (95% CI, 4%–47%), respectively. Median OS was inferior for male participants (HR, 5.5; 95% CI, 1.3–23; $P = 0.02$; Supplementary Table S4), and a trend toward improved median OS was noted for the eight participants who had prior radiotherapy to their primary anal tumor (HR, 0.34; 95% CI, 0.11–1.1; $P = 0.08$).

Adverse events/toxicity

There were seven participants (35%) who experienced a grade ≥3 treatment-related adverse event (**Table 2**), the most significant of which was a grade 5 bowel perforation. This occurred at the site of the patient's primary tumor in the distal colon/rectum and not from the anal mucosa. There were no preceding clinical signs or symptoms of immunotherapy-related colitis. Because the patient had presented with synchronous metastases of the liver and lung at the time of initial diagnosis, there had been no preceding administration of radiotherapy to the primary tumor before enrolling in this study. There were no high-risk features apparent other than bevacizumab, to which we can attribute the perforation at the primary tumor site.

Treatment with atezolizumab and bevacizumab was linked to grade 4 sepsis ($N = 1$) and hyponatremia (20%), hypertension

Table 2. Summary of adverse events.

Toxicity, number (%)	Grade 3	Grade 4	Grade 5
Abdominal pain	1 (5)		
Abscess	1 (5)		
Absolute lymphocyte count (decreased)	1 (5)		
Absolute neutrophil count (decreased)	1 (5)		
Anemia	1 (5)		
Bowel perforation			1 (5)
Encephalopathy	1 (5)		
Fistula	1 (5)		
Hypertension	2 (10)		
Infection	2 (10)		
Potassium (increased)	1 (5)		
Sepsis		1 (5)	
Sodium (decreased)	4 (20)		
Thromboembolic event	1 (5)		
Treatment-related MDS	1 (5)		

(10%), infection (10%), abdominal pain (5%), lymphopenia (5%), neutropenia (5%), anemia (5%), encephalopathy (5%), fistula formation (5%), hypercalcemia (5%), venous thromboembolism (5%), and treatment-related myelodysplastic syndrome (5%)—all grades 3. It was the same patient who developed an enterocutaneous fistula from the site of the previously irradiated anal tumor, which became colonized with bacteria from stool and led to infection with abscess development and sepsis. Adverse events across all grades are listed in Supplementary Table S5.

Dynamic gene expression signatures associated with survival

Genes demonstrating significant differential changes in expression, relative to baseline expression levels, following treatment with atezolizumab and bevacizumab were observed according to "favorable" or "unfavorable" PFS (defined as PFS greater than or less than 6 months, respectively; **Fig. 2A**) and OS (defined as OS greater than or less than 12 months, respectively; **Fig. 2B**). Prolonged PFS and OS alike were associated with posttreatment increased expression of *CYP4F11*, *EPHX2*, *FUCA1*, *FADH2A*, *AMT*, *OXER1*, *STAB2*, *DTX1*, *IL17RB*, *EYS*, and *GLS2* (Supplementary Fig. S1A). Alternatively, unfavorable survival outcomes for both PFS and OS correlated with increases in expression of genes linked with tumor suppression (*RPR15*, *PPPIR2*, and *PDCD5*), TGF-β regulation (*IRX3*), and centromere stabilization (*GGCT* and *CENPW*). Immunologic genes with increased expression after atezolizumab and bevacizumab that were associated with prolonged PFS (but not OS) included *EGR1* and *TNFRSF17* (Supplementary Fig. S1B). Expression in genes affecting antigen processing (*HLA-DMA*), chemokine signaling (*IL17RB*), T-cell regulation (*STAT4*), and NK cell function (*KLRC2*) was increased after atezolizumab and bevacizumab for those with prolonged OS (Supplementary Fig. S1C).

We evaluated pathways associated with prolonged survival according to relative changes in gene expression by comparing on- and pretreatment gene expression signatures. A PFS greater than 6 months was associated with an increase in immune activation gene signatures including "IFN-γ response" and "inflammatory response" (**Fig. 2C**). PFS less than 6 months was correlated with dynamic increases in "hypoxia," "p53 pathway," "DNA repair," "G2M checkpoint," and "E2F targeting" signatures. To investigate further the relative immune contributions, we applied bioinformatic analyses to evaluate specific immune cell signatures associated with survival outcomes. As seen in **Fig. 2D**, increases in "T-cell function," "B-cell function," and "NK cell function" were all observed in paired biopsies for participants with metastatic anal cancer experiencing longer PFS with atezolizumab and bevacizumab, whereas shorter PFS was linked to increases in "DNA damage repair" and "hypoxia signaling" signatures.

Similarly, prolonged OS beyond 12 months was associated with dynamic increases in immune signatures like "IFN-γ response," "allograft rejection," "complement," and "inflammatory response" (**Fig. 2E**). Unique immune cell gene expression signatures in this subgroup that significantly increased after study treatment included "B-cell function," "NK cell function," and "T-cell function," as well as "complement," "antigen processing," and "chemokine" signatures (**Fig. 2F**).

Changes in immune infiltrates with atezolizumab and bevacizumab

Paired tumor tissue collected from pre- and on-treatment biopsies was available for 10 study participants. In an exploratory analysis, we evaluated changes in immune biomarkers using mIF following treatment with atezolizumab and bevacizumab. Those with dynamic increases in proportions of $CD3^+CD8^+PD1^+$ T cells within the tumor microenvironment (**Fig. 3A** and **B** for representative pretreatment and on-treatment prevalence, respectively) experienced improved PFS (6.1 vs. 4.2 months; $P = 0.02$; **Fig. 3C**). Likewise, changes in $CD3^+FoxP3^+$ T cells from pre- and on-treatment samples were examined (**Fig. 3D** and **E**, respectively). In this study, decreases in $FoxP3^+CD3^+$ T cells in relation to $PD1^+CD3^+$ T cells were linked to prolonged PFS (8.5 vs. 4.2 months; $P = 0.04$; **Fig. 3F**).

Mutation profiling in relation to immunotherapy response

Whole-exome sequencing was performed on pretreatment biopsies. All tumors had multiple somatic alterations (**Fig. 4A**). Most variations were missense mutations (Supplementary Fig. S2A) although the majority of tumors had frameshift deletions. The median tumor mutation burden (TMB) was 6.6 mutations (IQR, 2.8) per megabase of DNA sequenced (Supplementary Fig. S2B). We evaluated any association between OS and TMB by comparing outcomes for patients with tumors harboring a TMB higher versus lower than the median TMB. As seen in Supplementary Fig. S2C, there was no significant PFS benefit for atezolizumab and bevacizumab linked with higher TMB (4.2 vs. 4.3 months; HR, 0.77; 95% CI, 0.28–2.1; $P = 0.60$), nor was there any difference in OS (10.7 vs. 11.7 months; HR, 0.63; 95% CI, 0.24–1.7; $P = 0.35$) according to TMB (Supplementary Fig. S2D).

We also analyzed these data according to the involved pathways for each mutation detected. Affected pathways with relevant mutations in at least 25% of anal cancers (Supplementary Fig. S3A) included NOTCH (90%), Hippo (85%), RTK-RAS (85%), Wnt (75%), PI3K (40%), Myc (25%), and TP53 (25%). For most of the tumors (Supplementary Fig. S3B), multiple aberrations for each pathway co-occurred and included alterations in oncogenes (blue) and tumor suppressor genes (red) alike.

Copy number variations linked to survival outcomes

Baseline tumor specimens collected from pretreatment biopsies were evaluated for copy-number changes (relative to germline sequencing of unaffected normal cells in matched patients). Overall, mRNA expression positively correlated with copy-number variations for the majority of genes sequenced (Supplementary Fig. S4A). For the samples analyzed for this clinical trial, anal cancers were

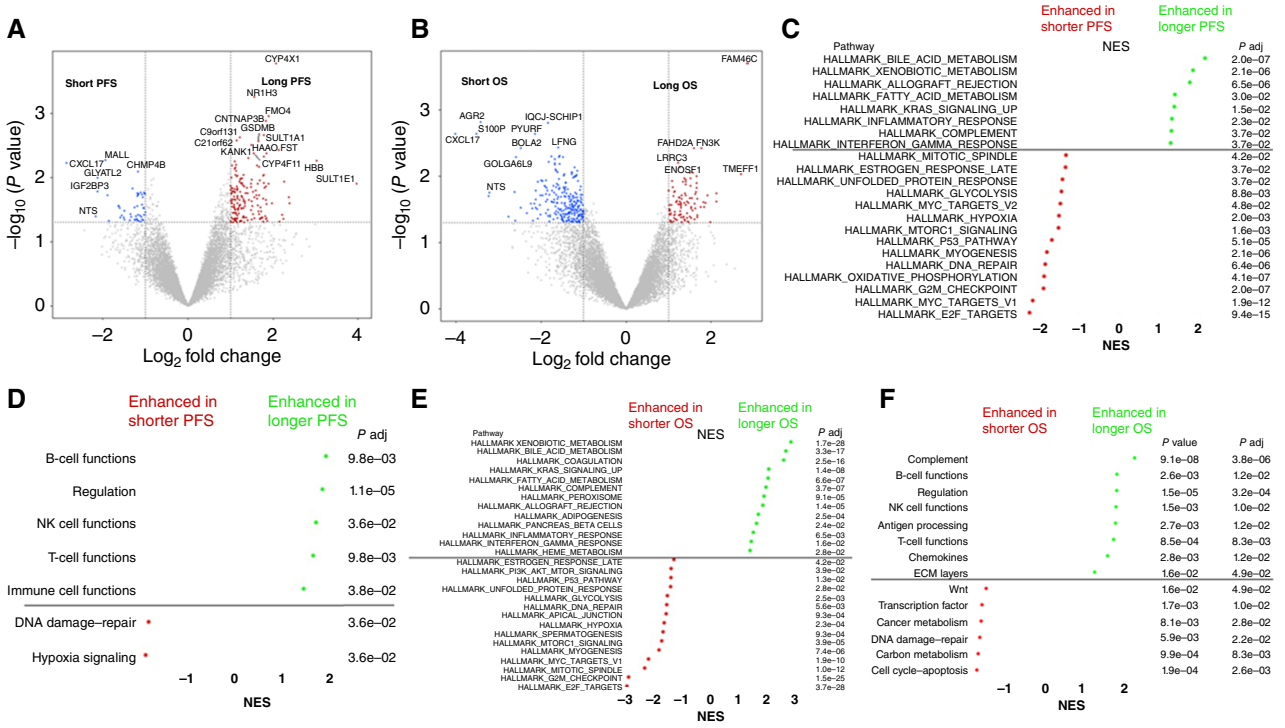

Figure 2.

Volcano plots for changes in gene expression according to PFS (**A**) and OS (**B**) and changes in normalized enrichment scores (NES) for Hallmark signatures and immune cell signatures for gene expression according to higher PFS (**C** and **D**) and OS (**E** and **F**) following treatment with atezolizumab and bevacizumab for metastatic anal cancer.

characterized by loss of 3p and 11q chromosome segments and gains in chromosome 3q (**Fig. 4B**). Based on these findings, we next evaluated any relationship between copy number change for individual genes and survival outcomes. Of interest, a group of genes on chromosome 4q with increased copy number was associated with significantly prolonged PFS and OS alike (Supplementary Fig. S4B). These included tumor suppressor genes such as *FBXW7*, *TET2*, and *FAT4*, and antitumor immune genes such as *IL2*.

SBS score as prognostic biomarker for metastatic anal cancer

Unsupervised clustering was performed from whole-exome sequencing data on baseline treatment specimens to evaluate differences in SBS signatures (Supplementary Fig. S5A). There were three clusters individually characterized by higher SBS-2 (activity of APOBEC; ref. 36), SBS31 (platinum chemotherapy treatment; ref. 37), and SBS-1 (clocklike signature; ref. 38), respectively (**Fig. 4C**). Mean (± SD) SBS31 scores were significantly higher for cluster 2 (0.60 ± 0.14; **Fig. 4D**) than for cluster 1 (0.24 ± 0.04; $P < 0.001$) and for cluster 3 (0.32 ± 0.11; $P = 0.003$). For these patients, despite no difference in median PFS (Supplementary Fig. S5B), cluster 2 seemed to be the least favorable prognostically (Supplementary Fig. S5C), with a significantly shorter median OS to atezolizumab and bevacizumab than the most favorable cluster 1 (19.2 vs. 7.6 months; HR, 6.3; 95% CI, 1.2–32; $P = 0.01$). To evaluate more specifically SBS31 as a prognostic biomarker, we compared median OS for patients with metastatic anal cancer above or below the median score. Although SBS31 was not associated with prolonged PFS (4.2 vs. 4.4 months; $P = 0.54$; 95% CI, 0.19–1.5) for study treatment (Supplementary Fig. S5D), a trend toward prolonged OS (**Fig. 4E**) was observed for the cohort with a lower SBS31 signature (15.3 vs. 10.1 months; HR, 0.4; 95% CI, 0.5–1.1; $P = 0.07$). Interestingly, when we evaluated survival outcomes according to whether participants did ($N = 10$) or did not ($N = 10$) experience tumor shrinkage with platinum chemotherapy prior to study participation, we did not observe any difference in PFS (4.2 vs. 4.3 months; HR, 0.34; 95% CI, 0.34–2.46; $P = 0.85$) or OS (12.1 vs. 9.6 months; HR, 0.65; 95% CI, 0.25–1.68; $P = 0.37$). This finding supports SBS31 as a potential unfavorable prognostic biomarker independent of clinical history for patients with metastatic anal cancer receiving immunotherapy.

Discussion

In this pilot, single-arm study of patients with unresectable and/or metastatic HPV-associated anal cancer, we observed clinical efficacy in a small number of patients using an immunotherapy combination targeting PD-L1 and VEGF. The addition of an anti-VEGF antibody to immune checkpoint blockade therapy did not seem to improve treatment outcomes relative to other clinical trials that have evaluated anti–PD-L1 antibodies as monotherapy for patients with previously treated metastatic anal cancer. In those studies (10–13), agents such as pembrolizumab, nivolumab, durvalumab, and retifanlimab were reported to have ORRs ranging between 10% and 24% and median PFS between 2 and 4 months. With an ORR of 11% and median PFS of 3.9 months, the addition of bevacizumab to immune checkpoint blockade does not seem to improve patient survival beyond historical precedent with anti–PD-L1 therapies alone or in combination with other targets for the treatment

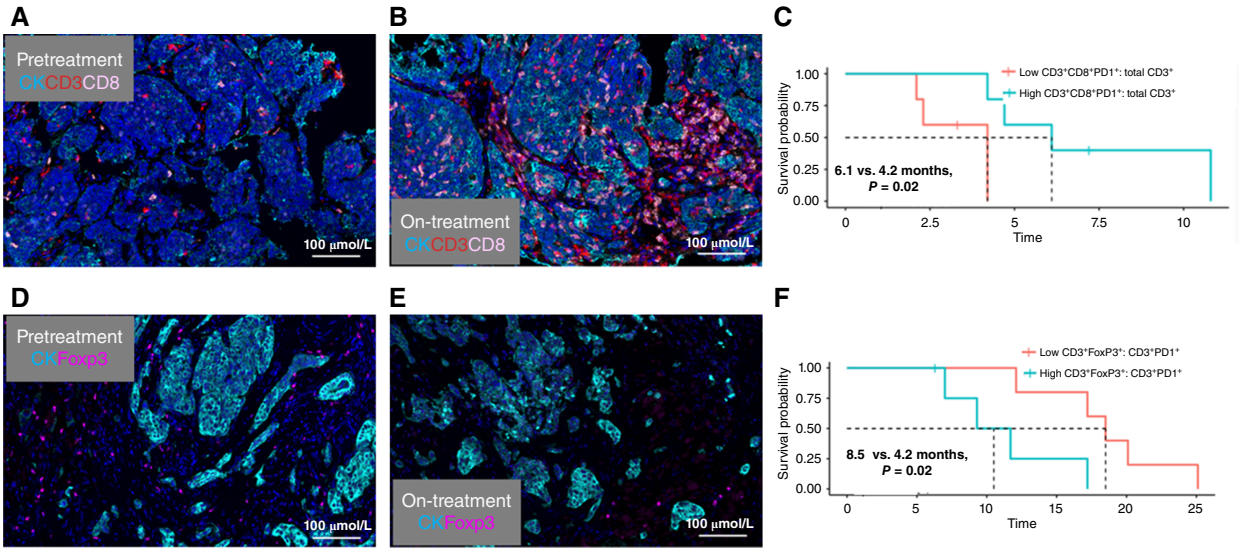

Figure 3.

mIF visualization of $CD3^+CD8^+$ cells increases from pretreatment (**A**) to on-treatment (**B**) biopsies in a tumor responding to treatment, consistent with favorable PFS for tumors with higher $CD3^+CD8^+PD1^+$ expression (**C**). Decreases from pretreatment (**D**) to on-treatment (**E**) tumor biopsies in a tumor responding to treatment, corresponding to improved PFS for lower expression of $CD3^+FoxP3^+$ cells (**F**).

of advanced/unresectable anal cancer. Treatment outcomes were further tempered by a side effect profile for grade 3 or higher treatment-related adverse events occurring in more than one third of study participants and notable for grade 5 bowel perforation and another with secondary myelodysplastic syndrome. Several grade 3+ toxicities such as abscess, infection, sepsis, and fistula that we observed here have not been reported as commonly in other phase III trials of other solid tumors treated with the same combination of atezolizumab and bevacizumab. However, these treatment-related AEs that we report in this study likely reflect the differing anatomic localization of the primary anal cancer within the stool-/bacteria-colonized distal gastrointestinal tract, which became susceptible to the infectious complications described.

Our work here is the first discovery-oriented analysis of paired biopsies of metastatic anal cancer collected prospectively for an immunotherapy clinical trial. Although other series had evaluated pretreatment biopsies only for associations with response to immunotherapy, we report for the first time dynamic changes within the tumor microenvironment by comparing biomarker signatures before and after treatment with atezolizumab and bevacizumab. In this study, we observed that prolonged survival outcomes were observed in those patients with tumors demonstrating increases in immune activation gene expression profiles—e.g., IFN-γ and inflammatory response profiles. These findings are consistent with previous reports that associated clinical benefit with immune checkpoint blockade to similar gene expression signatures of immune induction phenotype in other advanced solid tumors such as melanoma (39) and urothelial carcinoma (40). In a novel discovery, our data support a hypothesis that immunotherapy may effectively induce changes within the tumor microenvironment following treatment with atezolizumab and bevacizumab, which promote prolonged survival for patients with metastatic anal cancer. Gene expression signatures linked to specific immune cell types—not only T cells but also B cells and NK cells—were likewise increased after treatment preferentially in patients with greater survival benefit. Induction of multiple antitumor immune cell phenotypes beyond T cells, as supported by these findings, is a novel immune-based treatment approach that leverages B or NK cell–mediated cytotoxicity against advanced anal cancer and is thereby plausible.

Our mIF results further reinforce a hypothesis that immune activation within the tumor microenvironment correlates with improved outcomes with immunotherapy for patients with metastatic anal cancer. Recruitment of $PD1^+CD8^+$ cytotoxic T cells and reduction of $FoxP3^+$ (immune-suppressing) immune cells within the tumor microenvironment were observed for patients with PFS exceeding 6 months with atezolizumab and bevacizumab. This is a pattern of response with immune checkpoint blockade in other solid tumors but heretofore undescribed for metastatic anal cancer.

Although biomarkers associated with response to immunotherapy have been reported for anal cancer, in this study, most patients unfortunately did not experience therapeutic benefit from this combination of agents. Of interest, relative copy-number gains in *KDR*, *PDGFRα*, and *KIT* (all on chromosome 4q) were seen in more than half of the tumors of patients with better outcomes. Although targeting VEGF with bevacizumab alone did not seem effective, it is possible that these findings from these discovery-oriented analyses support further exploration of multikinase inhibitors that block these targets.

Characterization of negative prognostic biomarkers to immunotherapy remains poorly defined for incurable anal cancer. In this study, gene expression profiling demonstrated increases in the p53 and cell-cycle ("mitotic spindles," "G2M checkpoint," and "E2F targets") pathways linked to shorter survival outcomes following treatment with atezolizumab and bevacizumab in patients with metastatic anal cancer. Notably, these pathways are targets of the HPV oncoproteins E6 and E7, which promote aberrant tumor cell survival and proliferation via blockade of p53 (41) and Rb (42), respectively. Therefore, anal cancers characterized by increased

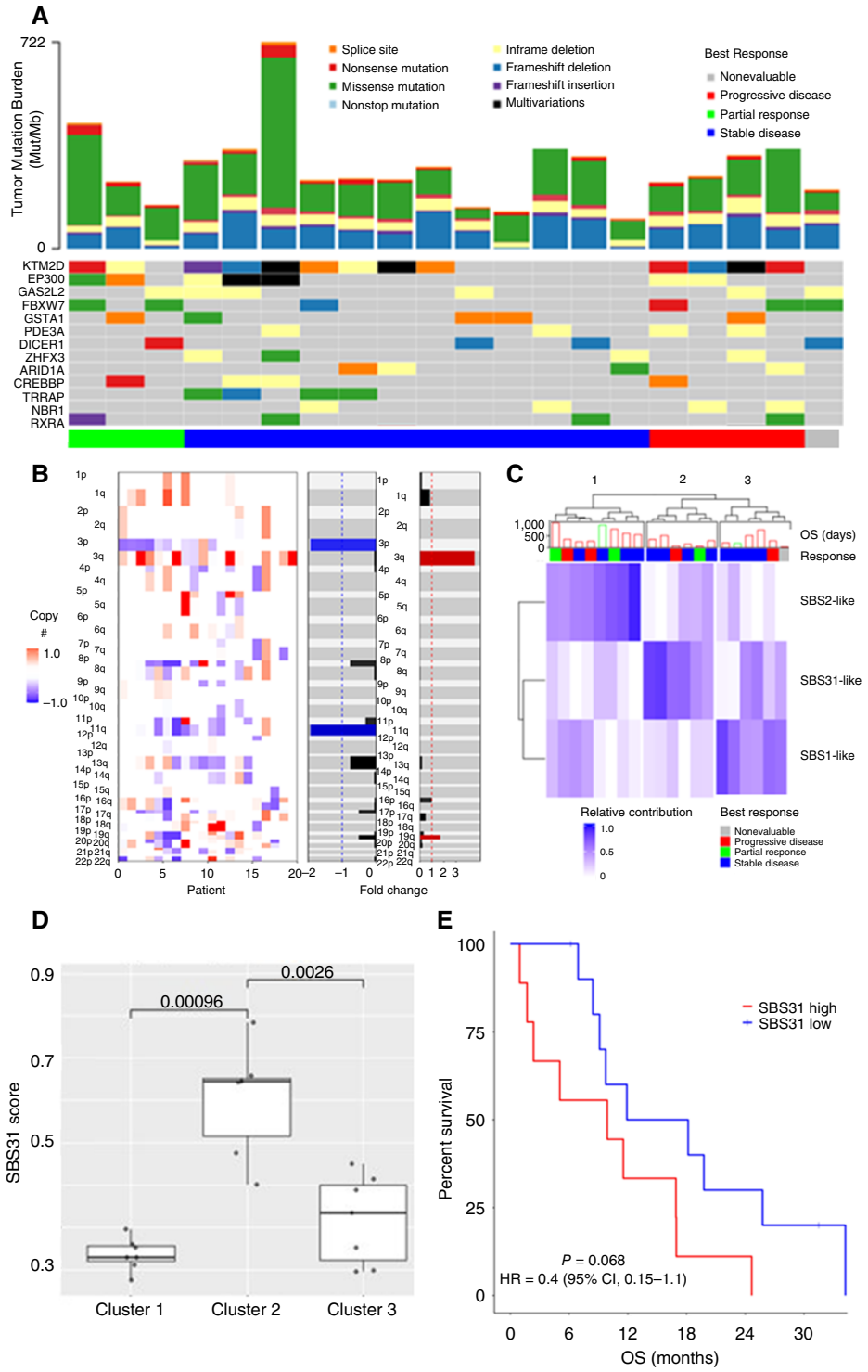

Figure 4.
Most commonly mutated genes (**A**) and chromosome alterations (**B**) for study participants; unsupervised clustering according to SBS signatures (**C**) reveals SBS31 as unique to cluster 2 (**D**) and OS (**E**) according to SBS31 signature.

activity of these known virally mediated oncogenic drivers may promote a lack of response to immunotherapy against HPV-positive anal cancer.

A higher TMB in our study was not linked to prolonged survival with atezolizumab and bevacizumab, consistent with the KEYNOTE-158 finding that reported no improvement in response to pembrolizumab for TMB high versus TMB low (7% vs. 11%, respectively; ref. 43). This finding was not surprising given the low tumor mutation burden intrinsic to anorectal squamous cell cancers (44). One novel finding from whole-exome sequencing was the identification of the SBS31 signature as a poor prognostic biomarker for patients with metastatic anal cancer treated with immunotherapy. It

is possible that this SBS31 signature, associated with exposure to prior platinum chemotherapy, may modulate the anal cancer microenvironment and predispose these tumors to a *de novo* lack of response to immunotherapy. Based upon a preceding phase II trial (45), the combination of carboplatin with paclitaxel is the most accepted first-line regimen for the treatment of metastatic/unresectable anal cancer, and relatively low rates of immunotherapy in the second-line setting and beyond, as reported here, may be influenced by prior receipt of platinum chemotherapy. Results from ongoing trials such as EA2176 (NCT04444921) and POD1UM-303 (NCT04472429) evaluating anti–PD-1 therapies in combination with cytotoxic chemotherapy doublets as first-line treatment for incurable anal cancer are awaited and may overcome this potential negative influence of prior chemotherapy in muting clinical benefit to immune checkpoint blockade.

We recognize the limitation that recruitment with a small cohort size to our single-institution clinical trial conducted at a large academic referral institution may not reflect the generalized population of patients diagnosed with metastatic anal cancer. Given the small sample size in this trial, it is possible that biomarkers reported in association with survival are prognostic in nature and do not predict response to targeted therapies against PD-L1 and VEGF together. We did collect biopsies from all study participants in this trial of an orphan malignancy, and analyses of paired biopsies, as reported here, offer novel insights heretofore unreported about the novel evolution of the anal cancer microenvironment following treatment with an immunotherapy combination, results confirmed even after correction for multiple comparisons.

In summary, the addition of bevacizumab to atezolizumab did not augment clinical benefit for patients with HPV-positive, unresectable, or metastatic anal cancer. Although considerable toxicity was noted for this combination, dual targeting of PD-L1 and VEGF does not seem to be an effective option in this context. Our findings do provide rationale, however, that support investigation of novel immunotherapy approaches for maximal promotion of immune activation to improve survival outcomes for patients with metastatic anal cancer.

Authors' Disclosures

V.K. Morris reports other support from Genentech during the conduct of the study as well as other support from Bristol Myers Squibb, Pfizer, Novartis, BioNTech, Sumitomo, Redx Pharma, Regeneron, and Scandion Oncology outside the submitted work. A. Mahvash reports grants and personal fees from Sirtex Medical and grants from Boston Scientific and Siemens outside the submitted work. I. Wistuba reports grants and personal fees from Genentech/Roche, Bayer, Bristol Myers Squibb, AstraZeneca, Pfizer, Merck, Novartis, Amgen, and Johnson and Johnson; personal fees from Guardant Health, Flame, Sanofi, Daiichi Sankyo, Jansen, Merus, G1 Therapeutics, AbbVie, Catalyst Therapeutics, Boehringer Ingelheim, Regeneron, Oncocyte, Medscape, and Platform Health; grants from Medimmune, Adaptimmune, EMD Serono, Takeda, Karus, Iovance, 4D, and Akoya outside the submitted work. J. Yao reports grants from Genentech during the conduct of the study as well as personal fees from HUTCHMED, Exelixis, TaiRx, and Sanofi outside the submitted work. S.E. Woodman reports other support from Genentech/Roche during the conduct of the study. D. Halperin reports grants from Genentech during the conduct of the study as well as grants and personal fees from Novartis, ITM, and Camurus; grants from Rayzebio; and personal fees from Exelixis, Chimeric Therapeutics, Crinetics, Lantheus, Harpoon Therapeutics, RadioMedix, and Amryt outside the submitted work. No disclosures were reported by the other authors.

Authors' Contributions

V.K. Morris: Conceptualization, resources, data curation, formal analysis, supervision, funding acquisition, investigation, methodology, writing–original draft, project administration, writing–review and editing. **S. Liu:** Conceptualization, data curation, formal analysis, investigation, methodology, writing–review and editing. **K. Lin:** Data curation, formal analysis, investigation, writing–review and editing. **H. Zhu:** Data curation, formal analysis, investigation, writing–review and editing. **S. Prasad:** Resources, supervision, writing–review and editing. **A. Mahvash:** Resources, data curation, writing–review and editing. **P. Bhosale:** Data curation, formal analysis, investigation, writing–review and editing. **B. Sun:** Resources, data curation, methodology, writing–review and editing. **E.R. Parra:** Conceptualization, data curation, investigation, methodology, writing–review and editing. **I. Wistuba:** Resources, investigation, methodology, writing–review and editing. **A. Peddireddy:** Data curation, investigation, writing–review and editing. **J. Yao:** Resources, investigation, visualization, methodology, writing–review and editing. **J. Mendoza-Perez:** Resources, project administration, writing–review and editing. **M. Knafl:** Data curation, software, formal analysis, supervision, investigation, methodology, writing–review and editing. **S.E. Woodman:** Conceptualization, data curation, software, formal analysis, supervision, validation, investigation, visualization, methodology, writing–review and editing. **C. Eng:** Conceptualization, resources, writing–review and editing. **D. Halperin:** Conceptualization, supervision, methodology, project administration, writing–review and editing.

Acknowledgments

We recognize with great appreciation our patients and their families/caregivers for participating in this study. We thank our MD Anderson team (Shaelynn Portier, Patricia Jensen-Loewe, April Vallian, Jawana Phillips, Alma Delagarza, Lori Manson, Kimberly Ross, Beryl Tross, and Nicole Rothschild) for assistance with clinical and translational research conduct and Betsy Williams for overseeing regulatory conduct for the MD Anderson–Genentech alliance. We recognize Dr. Jennifer Peterson for help with scientific editing. We acknowledge the Rare Cancer Initiative at MD Anderson for support with translational research performed on this study. We thank the members of the Translational Molecular Pathology Immune-Profiling Laboratory MoonShots Platform, specifically Beatriz Sanchez-Espiridion, Julia Mendoza, Shani Wijeratne, and Celia Garcia-Prieto for their assistance with sample procurement and inventory and Mei Jiang, Auriole Tamegnon, Heladio Ibarguem, Saxon Rodriguez, Renganayaki Krishna Pandurengan for their technical assistance. Funding support for this research was provided by F. Hoffmann-La Roche/Genentech and also by the NIH/NCI under award number K12 CA088084 (V.K. Morris), the Cancer Prevention and Research Institute of Texas (CPRIT) under award number RP220416 (V.K. Morris), the Andrew Sabin Fellow Family Foundation (V.K. Morris), and the University of Texas MD Anderson Cancer Center HPV Moon Shots Program (V.K. Morris).

Note

Supplementary data for this article are available at Clinical Cancer Research Online (http://clincancerres.aacrjournals.org/).

Received May 21, 2024; revised July 31, 2024; accepted February 26, 2025; posted first February 28, 2025.

References

1. De Vuyst H, Clifford GM, Nascimento MC, Madeleine MM, Franceschi S. Prevalence and type distribution of human papillomavirus in carcinoma and intraepithelial neoplasia of the vulva, vagina and anus: a meta-analysis. Int J Cancer 2009;124:1626–36.
2. Siegel RL, Miller KD, Wagle NS, Jemal A. Cancer statistics, 2023. CA Cancer J Clin 2023;73:17–48.
3. Deshmukh AA, Suk R, Shiels MS, Sonawane K, Nyitray AG, Liu Y, et al. Recent trends in squamous cell carcinoma of the anus incidence and mortality in the United States, 2001–2015. J Natl Cancer Inst 2020;112:829–38.
4. Frisch M, Glimelius B, van den Brule AJ, Wohlfahrt J, Meijer CJ, Walboomers JM, et al. Sexually transmitted infection as a cause of anal cancer. N Engl J Med 1997;337:1350–8.

5. Morris VK, Rashid A, Rodriguez-Bigas M, Das P, Chang G, Ohinata A, et al. Clinicopathologic features associated with human papillomavirus/p16 in patients with metastatic squamous cell carcinoma of the anal canal. Oncologist 2015;20:1247–52.
6. Faivre C, Rougier P, Ducreux M, Mitry E, Lusinchi A, Lasser P, et al. [5-fluorouracile and cisplatinum combination chemotherapy for metastatic squamous-cell anal cancer]. Bull Cancer 1999;86:861–5.
7. Ajani JA, Carrasco CH, Jackson DE, Wallace S. Combination of cisplatin plus fluoropyrimidine chemotherapy effective against liver metastases from carcinoma of the anal canal. Am J Med 1989;87:221–4.
8. Eng C, Chang GJ, You YN, Das P, Rodriguez-Bigas M, Xing Y, et al. The role of systemic chemotherapy and multidisciplinary management in improving the overall survival of patients with metastatic squamous cell carcinoma of the anal canal. Oncotarget 2014;5:11133–42.
9. Mondaca S, Chatila WK, Bates D, Hechtman JF, Cercek A, Segal NH, et al. FOLFCIS treatment and genomic correlates of response in advanced anal squamous cell cancer. Clin Colorectal Cancer 2019;18:e39–52.
10. Marabelle A, Cassier PA, Fakih M, Guren TK, Italiano A, Kao SC-H, et al. Pembrolizumab for advanced anal squamous cell carcinoma (ASCC): results from the multicohort, phase II KEYNOTE-158 study. J Clin Oncol 2020; 38(Suppl 4):1.
11. Morris VK, Salem ME, Nimeiri H, Iqbal S, Singh P, Ciombor K, et al. Nivolumab for previously treated unresectable metastatic anal cancer (NCI9673): a multicentre, single-arm, phase 2 study. Lancet Oncol 2017;18:446–53.
12. Rao S, Anandappa G, Capdevila J, Dahan L, Evesque L, Kim S, et al. A phase II study of retifanlimab (INCMGA00012) in patients with squamous carcinoma of the anal canal who have progressed following platinum-based chemotherapy (POD1UM-202). ESMO Open 2022;7:100529.
13. Lonardi S, Prete AA, Morano F, Messina M, Formica V, Corsi DC, et al. Randomized phase II trial of avelumab alone or in combination with cetuximab for patients with previously treated, locally advanced, or metastatic squamous cell anal carcinoma: the CARACAS study. J Immunother Cancer 2021;9:e002996.
14. Ferrara N, Gerber HP, LeCouter J. The biology of VEGF and its receptors. Nat Med 2003;9:669–76.
15. Willett CG, Boucher Y, di Tomaso E, Duda DG, Munn LL, Tong RT, et al. Direct evidence that the VEGF-specific antibody bevacizumab has antivascular effects in human rectal cancer. Nat Med 2004;10:145–7.
16. Simons M, Gordon E, Claesson-Welsh L. Mechanisms and regulation of endothelial VEGF receptor signalling. Nat Rev Mol Cell Biol 2016;17:611–25.
17. Manning EA, Ullman JG, Leatherman JM, Asquith JM, Hansen TR, Armstrong TD, et al. A vascular endothelial growth factor receptor-2 inhibitor enhances antitumor immunity through an immune-based mechanism. Clin Cancer Res 2007;13:3951–9.
18. Kusmartsev S, Eruslanov E, Kübler H, Tseng T, Sakai Y, Su Z, et al. Oxidative stress regulates expression of VEGFR1 in myeloid cells: link to tumor-induced immune suppression in renal cell carcinoma. J Immunol 2008;181:346–53.
19. Roland CL, Lynn KD, Toombs JE, Dineen SP, Udugamasooriya DG, Brekken RA. Cytokine levels correlate with immune cell infiltration after anti-VEGF therapy in preclinical mouse models of breast cancer. PLoS One 2009;4:e7669.
20. CTCAE version 4.03. [cited 2025 March 12]. Available: http://nciterms.nci.nih.gov/ncitbrowser/pages/vocabulary.jsf?dictionary=Common%20Terminology%20Criteria%20for%20Adverse%20Events.
21. Dobin A, Davis CA, Schlesinger F, Drenkow J, Zaleski C, Jha S, et al. STAR: ultrafast universal RNA-seq aligner. Bioinformatics 2013;29:15–21.
22. Anders S, Pyl PT, Huber W. HTSeq–a Python framework to work with high-throughput sequencing data. Bioinformatics 2015;31:166–9.
23. Liberzon A, Birger C, Thorvaldsdóttir H, Ghandi M, Mesirov JP, Tamayo P. The Molecular Signatures Database (MSigDB) hallmark gene set collection. Cell Syst 2015;1:417–25.
24. Zack TI, Schumacher SE, Carter SL, Cherniack AD, Saksena G, Tabak B, et al. Pan-cancer patterns of somatic copy number alteration. Nat Genet 2013;45:1134–40.
25. Li H, Durbin R. Fast and accurate short read alignment with Burrows-Wheeler transform. Bioinformatics 2009;25:1754–60.
26. DePristo MA, Banks E, Poplin R, Garimella KV, Maguire JR, Hartl C, et al. A framework for variation discovery and genotyping using next-generation DNA sequencing data. Nat Genet 2011;43:491–8.
27. Andrews MC, Oba J, Wu CJ, Zhu H, Karpinets T, Creasy CA, et al. Multimodal molecular programs regulate melanoma cell state. Nat Commun 2022; 13:4000.
28. Cibulskis K, Lawrence MS, Carter SL, Sivachenko A, Jaffe D, Sougnez C, et al. Sensitive detection of somatic point mutations in impure and heterogeneous cancer samples. Nat Biotechnol 2013;31:213–9.
29. Ye K, Schulz MH, Long Q, Apweiler R, Ning Z. Pindel: a pattern growth approach to detect break points of large deletions and medium sized insertions from paired-end short reads. Bioinformatics 2009;25:2865–71.
30. Wang K, Li M, Hakonarson H. ANNOVAR: functional annotation of genetic variants from high-throughput sequencing data. Nucleic Acids Res 2010;38: e164.
31. Ha G, Roth A, Lai D, Bashashati A, Ding J, Goya R, et al. Integrative analysis of genome-wide loss of heterozygosity and monoallelic expression at nucleotide resolution reveals disrupted pathways in triple-negative breast cancer. Genome Res 2012;22:1995–2007.
32. Mermel CH, Schumacher SE, Hill B, Meyerson ML, Beroukhim R, Getz G. GISTIC2.0 facilitates sensitive and confident localization of the targets of focal somatic copy-number alteration in human cancers. Genome Biol 2011;12:R41.
33. Favero F, Joshi T, Marquard AM, Birkbak NJ, Krzystanek M, Li Q, et al. Sequenza: allele-specific copy number and mutation profiles from tumor sequencing data. Ann Oncol 2015;26:64–70.
34. Manders F, Brandsma AM, de Kanter J, Verheul M, Oka R, van Roosmalen MJ, et al. MutationalPatterns: the one stop shop for the analysis of mutational processes. BMC Genomics 2022;23:134.
35. Parra ER, Ferrufino-Schmidt MC, Tamegnon A, Zhang J, Solis L, Jiang M, et al. Immuno-profiling and cellular spatial analysis using five immune oncology multiplex immunofluorescence panels for paraffin tumor tissue. Sci Rep 2021;11:8511.
36. Swanton C, McGranahan N, Starrett GJ, Harris RS. APOBEC enzymes: mutagenic fuel for cancer evolution and heterogeneity. Cancer Discov 2015;5:704–12.
37. Pleasance E, Titmuss E, Williamson L, Kwan H, Culibrk L, Zhao EY, et al. Pan-cancer analysis of advanced patient tumors reveals interactions between therapy and genomic landscapes. Nat Cancer 2020;1:452–68.
38. Alexandrov LB, Jones PH, Wedge DC, Sale JE, Campbell PJ, Nik-Zainal S, et al. Clock-like mutational processes in human somatic cells. Nat Genet 2015; 47:1402–7.
39. Grasso CS, Tsoi J, Onyshchenko M, Abril-Rodriguez G, Ross-Macdonald P, Wind-Rotolo M, et al. Conserved interferon-gamma signaling drives clinical response to immune checkpoint blockade therapy in melanoma. Cancer Cell 2020;38:500–15 e3.
40. Ayers M, Lunceford J, Nebozhyn M, Murphy E, Loboda A, Kaufman DR, et al. IFN-gamma-related mRNA profile predicts clinical response to PD-1 blockade. J Clin Invest 2017;127:2930–40.
41. Werness BA, Levine AJ, Howley PM. Association of human papillomavirus types 16 and 18 E6 proteins with p53. Science 1990;248:76–9.
42. Balsitis SJ, Sage J, Duensing S, Münger K, Jacks T, Lambert PF. Recapitulation of the effects of the human papillomavirus type 16 E7 oncogene on mouse epithelium by somatic Rb deletion and detection of pRb-independent effects of E7 in vivo. Mol Cell Biol 2003;23:9094–103.
43. Marabelle A, Fakih M, Lopez J, Shah M, Shapira-Frommer R, Nakagawa K, et al. Association of tumour mutational burden with outcomes in patients with advanced solid tumours treated with pembrolizumab: prospective biomarker analysis of the multicohort, open-label, phase 2 KEYNOTE-158 study. Lancet Oncol 2020;21:1353–65.
44. Morris V, Rao X, Pickering C, Foo WC, Rashid A, Eterovic K, et al. Comprehensive genomic profiling of metastatic squamous cell carcinoma of the anal canal. Mol Cancer Res 2017;15:1542–50.
45. Rao S, Sclafani F, Eng C, Adams RA, Guren MG, Sebag-Montefiore D, et al. International rare cancers initiative multicenter randomized phase II trial of cisplatin and fluorouracil versus carboplatin and paclitaxel in advanced anal cancer: InterAAct. J Clin Oncol 2020;38:2510–8.